Available online at www.sciencedirect.com
SCIENCE DIRECT
Journal of Molecular Catalysis A: Chemical 248 (2006) 76–83
JOURNAL OF MOLECULAR CATALYSIS A: CHEMICAL
www.elsevier.com/locate/molcata

Adsorption of 1-hexene on γ-alumina (110C)

Shuhui Cai [a,b], Karl Sohlberg [b,*]

[a] Department of Physics, State Key Laboratory of Physical Chemistry of Solid Surface, Xiamen University, Xiamen 361005, PR China
[b] Department of Chemistry, Drexel University, Philadelphia, PA 19104, USA

Received 24 October 2005; received in revised form 22 November 2005; accepted 22 November 2005
Available online 19 January 2006

Abstract

Adsorption of 1-hexene on the γ-alumina (110C) surface is investigated with semi-empirical (PM3) cluster calculations. It is found that on the Al–O terminated surface, H-abstraction to surface oxygen from the hexene allylic position is the most favorable reaction, and is facilitated by C–Al interaction. Hexene interactions with surface aluminum atoms are purely repulsive. Except for the pure H-abstraction, chemisorption occurs through interactions of C and H with surface oxygen atoms, which is typically an endothermic process but is most favorable when an H is abstracted from the hexene allylic position accompanied by the formation of a C–O bond, and becomes exothermic when there is an associated transfer of a surface H. On the oxygen-terminated surface, numerous different types of H atoms on hexene can be abstracted by surface oxygen when they come sufficiently close to the surface and these reactions are exothermic. The energy barriers to these different H-abstraction processes are all in the range 10–15 kcal/mol, with those for the dehydrogenation of a terminal H farthest from the double bond or an allylic H being slightly lower than those for abstracting H from other positions. The comparable energy barriers for abstraction of numerous different kinds of H provide a possible explanation for the experimentally observed plethora of products.

Keywords: Chemisorption; 1-Hexene; Cracking; Semi-empirical calculations; γ-Alumina

1. Introduction

Aluminas have been used extensively as adsorbents, active catalysts and catalytic supports [1,2]. The studies of Tung and Mcininch (TM) on the activity of high-purity alumina for 1-hexene conversion reactions showed that high-purity alumina possesses fairly good activity for 1-hexene cracking above 400 °C [3,4]. A plethora of products is produced. The observed gaseous cracking pattern of 1-hexene on alumina was explained by assuming the presence of two types of acid sites on alumina surfaces: Lewis acid sites; passive Bronsted acid sites. It was proposed that on alumina at 450 °C, hexene first cracks upon Lewis acid sites via a carbonium ion mechanism to form site-bound olefins [3,4]. These, in turn, combine with hydrogen atoms to yield site-bound radicals. Further cracking then occurs via a free radical mechanism. Denoting the Lewis acid sites by L^+, cracking of hexene by this TM mechanism [3,4] may be, in part, formally represented by Scheme 1.

By contrast, in a study of skeletal isomerization of *n*-butene on alumina, Trombetta et al. suggested that C_4 olefins interact at room temperature with surface hydroxy groups on alumina (Scheme 2) [5]. Additionally, they suggested that olefins dissociate over Al^{3+}–O^{2-} "acidic" couples, giving rise to allyl species that are nearly covalently bonded to surface aluminum atoms (Scheme 3) [5]. It was further suggested that at higher temperature, strongly bonded carbonaceous species grow on the surface at the expense of the allyl species. (Two strong IR bands, at 1570 and 1480 cm^{-1}, provided evidence of the presence of carboxylates.) This is quite different from the proposal of Tung and McInnich [3,4]. A complete description of olefin interactions with alumina, in particular the roles of the surface acid and base sites, has not been definitively established. Such an atomic scale understanding would be of considerable value in the design of improved catalysts.

Most previous theoretical investigations of adsorption on γ-alumina focused on the Lewis acidity of surface Al sites [6–8]. Their reactivity with water [9–11], hydrogen sulfide [9], carbon monoxide [9], ammonia [10], pyridine [10], and methanol [12] has been studied. Previous investigations by the present authors considered alcohol adsorption on γ-alumina [13].

* Corresponding author. Tel.: +1 215 895 2653; fax: +1 215 895 1265.
E-mail address: sohlbergk@drexel.edu (K. Sohlberg).

1381-1169/$ – see front matter © 2005 Elsevier B.V. All rights reserved.
doi:10.1016/j.molcata.2005.11.059

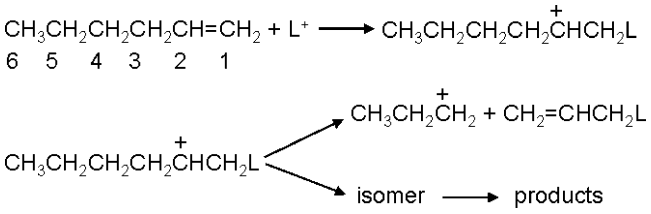

Scheme 1.

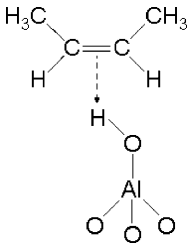

Scheme 2.

Herein, we report the results of calculations designed to investigate the preferred adsorption sites for 1-hexene on γ-alumina (110C) surfaces. Two cluster models, $H_8Al_{40}O_{64}$ (which exposes an Al–O terminated face) and $H_{10}Al_{50}O_{80}$ (which exposes an oxygen-terminated face), were used to model the γ-alumina surface. These surface models include all atoms up to and including second-nearest neighbors of the adsorption site. We found that on the $H_8Al_{40}O_{64}$ model, the most preferable first reaction step is H-abstraction from the hexene allylic position. By contrast, the direct reaction of the C1 or C2 atom (see Scheme 1 for atomic labeling) with a Lewis acid site is found to be purely repulsive. On the $H_{10}Al_{50}O_{80}$ model, H atoms can be abstracted from numerous positions on hexene by surface oxygen when they come sufficiently close to the surface. The energy barriers to these different H-abstraction processes are comparable (around 10–15 kcal/mol) with those for the dehydrogenation of a terminal H beyond the double bond or an allylic H being slightly lower than those for abstracting H from other positions. This result offers a possible explanation for the plethora of experimentally observed reaction products.

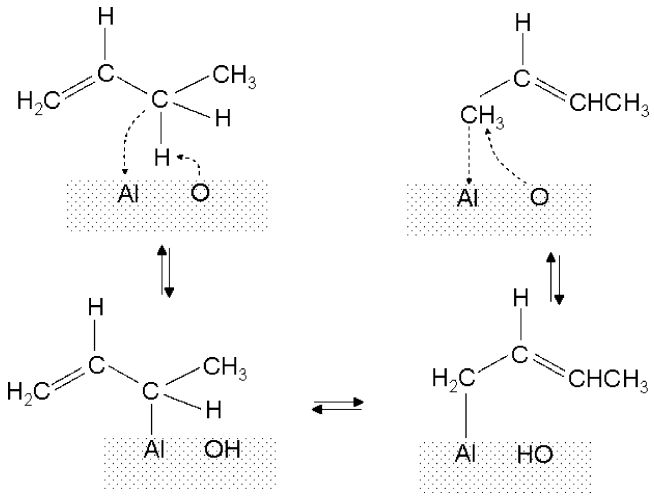

Scheme 3.

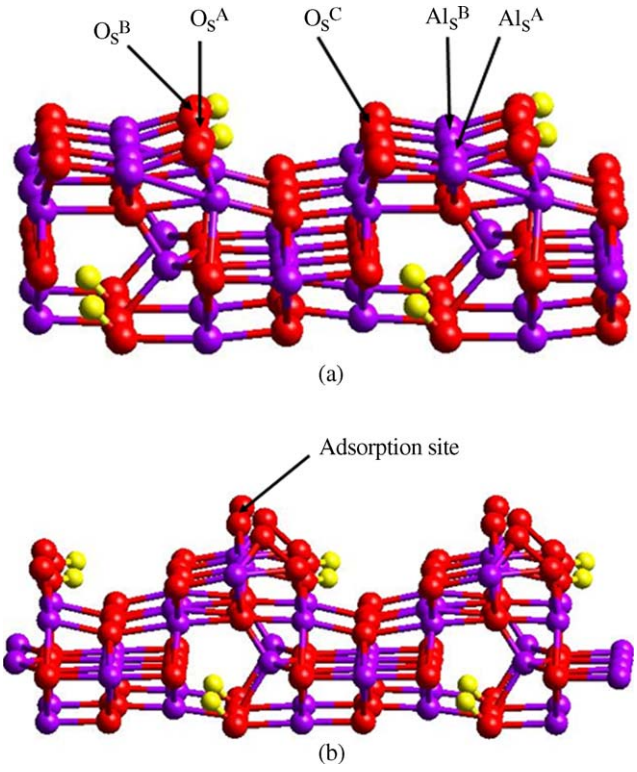

Fig. 1. Cluster models used in this study. (a) Model I—an Al–O terminated surface; (b) Model II—an oxygen-terminated surface. The purple, red and yellow spheres represent Al, O, and H atoms, respectively.

2. Computational method and models

The adsorption of 1-hexene on the γ-alumina (110C) surface was investigated with electronic structure calculations based on the semi-empirical PM3 Hamiltonian [14,15] and $H_8Al_{40}O_{64}$ and $H_{10}Al_{50}O_{80}$ cluster models of γ-alumina (see Fig. 1). Semi-empirical models have been used effectively in theoret-

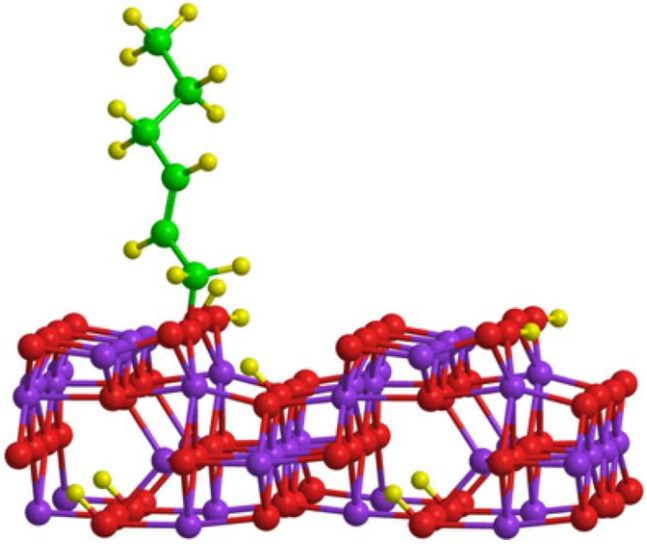

Fig. 3. The final optimized geometry of the reaction of C1–O_s^A + H3–O_s^B on Model I. The purple, red, green, and yellow spheres represent Al, O, C, and H atoms, respectively.

ical investigations of similar systems, including adsorptions on metal oxide surfaces [7,13,16,17]. They have been shown to lead to qualitative conclusions and energetic behavior consistent with ab initio calculations. For example, a comparison of the binding energies for several low-molecular weight alcohols on the alumina surface as predicted by PM3 and ab initio calculations showed an RMS difference of only 5.7% (see also, Refs. [7,13,18–21]). The much lower computational cost of semi-empirical calculations allows for modeling a cluster that includes all atoms up to and including second-nearest neighbors of the adsorption site, much larger than is currently practical with first-principles methods.

γ-Alumina has been described as a defect spinel structure closely related to that of Mg-spinel (space group $Fd\bar{3}m$) [22] and aluminum cations are distributed over the octahedral (O_h, Al sites) and tetrahedral (T_d, Mg sites) interstitial sites within the oxygen anion sublattice. γ-Alumina has a range of valid stoichiometries $H_{3m}Al_{2-m}O_3$ ($0 \leq m \leq 1/3$), but the lowest energy form has the stoichiometry of a hydrogen–aluminum spinel [23]. The primitive unit cell of the lowest energy form is HAl_5O_8, where the H atom and one Al atom occupy (nominally) the Mg sites in the spinel structure, and the remaining four Al atoms occupy the Al sites in the spinel structure. Surface studies show that the (110C) layer of γ-alumina is preferentially exposed [1,24–26]. While simple cleavage of bulk γ-alumina will produce both three-coordinated Al (those at T_d sites) and four-coordinated Al (those at O_h sites) at the (110C) surface, a spontaneous reconstruction depletes the three-coordinated Al from the surface [26,27], and only four-coordinated Al are observed [28]. Based on structural relaxation studies of a 56-atom slab of γ-alumina four atomic layers thick [29], the $H_8Al_{40}O_{64}$ cluster model (Model I) was constructed. In addition, it has been suggested that alumina surfaces are plausibly anion terminated [1]. Oxygen termination is accomplished by bridging adjacent O_h (four-coordinated) Al atoms on the surface with Al–O–Al structures. The $H_{10}Al_{50}O_{80}$ cluster model (Model II) was constructed based on the full structural relaxation with the "extra" terminating row of oxygen atoms [30]. These two models ensure that the coordination environment of the surface atoms interacting with the adsorbate, and their nearest neighbors, are representative of those on the surface of the periodic crystal.

For Model I, only surface Al atoms at O_h sites were considered to interact with hexene carbon since three-coordinated Al practically does not exit on the surface [26–28]. Two different surface aluminum sites for hexene adsorption were studied as indicated in Fig. 1(a). At site A, the surface Al atom interacting with the hexene (Lewis acid site, which we denote Al_s^A. The subscript "s" indicates an atom on the alumina surface. A surface Lewis acid site is Al_s, a surface Lewis base site is O_s.) has a neighboring OH. At site B, there is no neighboring OH around the Al atom that interacts with hexene (denoted as Al_s^B). Interactions of hexene with three different surface O sites were considered as indicated in Fig. 1(a). At site A, the surface O atom is coordinated by one H atom and two Al atoms (denoted as O_s^A). At site B, the surface O atom is coordinated by two Al atoms (denoted as O_s^B). At site C, the surface O atom is coordinated by three Al atoms (denoted as O_s^C). As previous density-functional calculations have shown no appreciable relaxation effects or consequence for surface atoms, excluding the three-coordinated Al not considered here [26], the alumina substrate was frozen in all calculations with the exception of the H atom bound to the O_s^A atom.

For Model II, interactions of H from different carbon positions on hexene with a surface oxygen atom on the oxygen-terminating row were considered (see Fig. 1(b)).

In structural optimizations, the adsorbed molecules were fully relaxed, including their positions relative to the surface, except for the cases explicitly noted otherwise. For all chemisorbed states, vibrational frequencies were calculated to ensure that each state is a true local minimum. (The number of real vibrational frequencies must equal the number of degrees of freedom exclusive of those in the frozen slab, less six for overall translations and vibrations.) Vibrational frequencies were identified by animation of the computed normal mode vibrational motions and their numerical values were scaled by a factor of 0.9761 as is recommended for PM3 calculations [31].

The following possible interaction modes were investigated on Model I: (1) a C atom or C=C double bond interacts with a surface Lewis acid site (C–Al_s); (2) the C=C double bond, or a C atom interacts with a surface hydroxy group (as Scheme 2 or C–H_s); (3) a C atom interacts with a surface Lewis base site (C–O_s); (4) a H atom of hexene interacts with a surface Lewis base site (H–O_s); (5) other chemically reasonable interactions involving a multi-center structure whereby a C atom interacts with a surface Lewis acid site (C–O_s) or base site (C–Al_s) and a H atom of hexene interacts with a surface Lewis base site (H–O_s), or there is another C–O_s interaction.

3. Results and discussion

3.1. Adsorption of hexene on Model I

3.1.1. Interactions of C with surface Al atoms

First, we studied adsorption configurations in which the C1 (or C2) atom of hexene interacts with a surface aluminum atom Al_s. The initial C1–Al_s (or C2–Al_s) distance is set to 0.14 nm to allow strong interaction. After full optimization, including the C1 and C2 position relative to the surface, the molecule leaves the surface without any reaction. Fixing the C1 (or C2) atom at various positions and relaxing all other atoms of the molecule, the energy variation with the C1–Al_s (or C2–Al_s) distance can be mapped out, as shown in Fig. 2, where $\Delta E = E(\text{hexene}/H_8Al_{40}O_{64}) - E(\text{hexene}) - E(H_8Al_{40}O_{64})$. It can be seen that the interaction between C1 (or C2) and Al is repulsive, increasing rapidly with decreasing C1–Al_s (or C2–Al_s) distance. The interactions of Al_s^A and Al_s^B with C1 (or C2) are very similar, with the C2–Al_s interaction being slightly stronger than C1–Al_s. For example, the energy increase for a free molecule to come to a position with d(C–Al_s) = 0.20 nm is 97, 98, 121, and 126 kcal/mol for the cases of C1–Al_s^A, C1–Al_s^B, C2–Al_s^A, and C2–Al_s^B, respectively. It is interesting to note that when d(C–Al_s) = 0.14 nm, H2 is dehydrogenated in the case of C2–Al_s^A interaction. Even in such case, however, the energy of the final state is much higher than that of the non-dehydrogenated

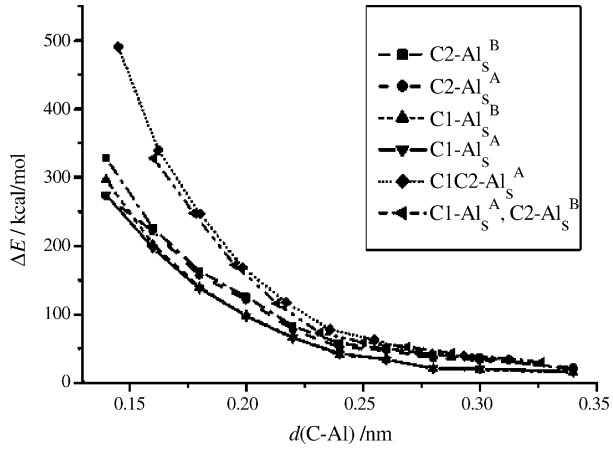

Fig. 2. Energy variations with C–Al_s distance for hexene interactions with Model I. All d(C–Al) are d(C1–Al_s^A) except for the cases marked C1–Al_s^B and C2–Al_s^B. Symbols indicate the computed points.

state. As shown in Fig. 2, the energy increases monotonically with decreasing C–Al_s distance. The dehydrogenation is an artifact of the constrained C2–Al_s^A distance. If the whole molecule is relaxed, no dehydrogenation happens; it is simply repelled from the surface.

We also studied the adsorption configuration in which the C1 and C2 atoms are brought close to Al_s^A simultaneously, or C1 is brought close to Al_s^A and C2 close to Al_s^B, respectively. The C=C bond is not completely parallel to the surface in either case. For the former case, the projection of the C=C bond on the surface is slightly deviated from the Al_s^A–Al_s^B direction and Al_s^A is nearly the center of the projection. If the molecule is fully relaxed, it will leave the surface and no chemisorption happens. Fixing the C1 and C2 atoms at different positions and relaxing all other atoms of the molecule, the energy variations with the C1–Al_s (or C2–Al_s) distance were also calculated. The results are shown in Fig. 2, where the C–Al distances are for C1–Al_s^A. The interactions between C and Al for these two cases are comparable, and they are stronger than a single C–Al_s interaction. For example, the energy increase for a free molecule to come to such a surface position with d(C–Al_s) = 0.20 nm is 169 and 172 kcal/mol for the cases of C1C2–Al_s^A, and C1–Al_s^A, C2–Al_s^B, respectively. When d(C–Al_s) = 0.16 nm, H1 is dehydrogenated in the case of the C1–Al_s^A, C2–Al_s^B interaction. As is the case for the C2–Al_s^A interaction, however, the energy of such a final state is much higher than that of the corresponding non-dehydrogenated state.

The above results imply that the first step of hexene cracking is not due to a double bond-related interaction of hexene with a surface Lewis acid site (Scheme 1).

3.1.2. Interactions of C with a surface H atom

Three cases of C–H_s interactions were considered: the interaction of C1 with a surface H atom, the interaction of C2 with a surface H atom, and the interaction of both C1 and C2 with a surface H atom. The third case is similar to Scheme 2. For all cases, the molecule is placed close to the surface so that the specific C–H_s distance(s) is(are) ≈0.1 nm. No bond between H_s and hexene forms when the molecule is relaxed. The molecule simply leaves the surface without any reaction, indicating that abstraction of H_s atoms from the surface OH by hexene is unlikely without additional external force. This result is consistent with the general rule that O–H bonds are greater in strength than C–H bonds [32]. We would expect that breaking an OH bond to form a CH bond would be energetically unfavorable.

3.1.3. Interactions of C with a surface O atom

The interactions of C1 (or C2) with a surface oxygen O_s (sites A, B, or C) were investigated. The C1–O_s (or C2–O_s) distance was set to be ≤0.15 nm and the molecule was subjected to full structural optimization, including the C–O_s distance. It was found that C1 or C2 remains bound only to O_s^C after the molecule is relaxed, whereupon d(C1–O_s^C) = 0.142 nm or d(C2–O_s^C) = 0.153 nm. The energies of these final chemisorbed states, however, are higher than that of the corresponding free state [E(hexene) + E($H_8Al_{40}O_{64}$)], by 84 and 105 kcal/mol, respectively.

3.1.4. Interactions of H with a surface O atom

The interactions of H1, H2, H3, or H6 (the number refers to the labeling of C atoms) with a surface oxygen O_s (sites A, B, or C) were investigated using trial configurations with the H–O_s distance ≈ 0.1 nm. No reactions were found. In all cases, upon full structural optimization the molecule simply relaxed away from the surface.

3.1.5. Simultaneous interactions of C and H to surface O atoms

Next we considered configurations that bring C and H close to different O_s atoms. The initial distances between C–O_s and H–O_s were set to d(C1–O_s) ≈ 0.14–0.17 nm and d(H1–O_s) ≈ 0.097–0.12 nm. The results of full structural optimization are listed in Table 1. When the initial configuration places C1 close to O_s^A (or O_s^B) and H1 close to O_s^B (or O_s^A), no reactions happen. When C1 and H1 are placed close to two nearby O_s^C sites, however, C1 remains bound to O_s^C after structural optimization. When C1 is placed close to an O_s and H2 close to another O_s (the two O_s can be any combination of O_s^A, O_s^B, and O_s^C except for the pair of O_s^A and O_s^C), a C1–O_s bond forms and H2 transfers to O_s. No reactions happen on the pair of O_s^A and O_s^C. When C1 is placed close to an O_s and H3 close to another O_s (the two O_s can be any combination of O_s^A, O_s^B, and O_s^C), upon structural relaxation a C1–O_s bond forms and H3 transfers to O_s (Fig. 3). When C2 is placed close to O_s^A and H2 close to O_s^B, no reactions happen. When C2 is placed close to O_s^B (or O_s^C) and H2 close to O_s^A (or O_s^C), C2 bonds to O_s^B (or O_s^C) and H2 transfers to O_s^A (or O_s^C). When C2 is placed close to O_s^C and H3 close to any O_s, C1 (not C2) bonds to O_s^C and H3 transfers to O_s, which is similar to the cases where C1 and H3 interact with O_s.

Note that for some of the above reactions, the H_s originally bonded to O_s^A moves to a nearby O_s if O_s^A is involved in reaction due to strong repulsive interaction between H_s and nearby C or H atoms in the initial state. As shown in Table 1, this typically has the effect of significantly decreasing ΔE for chemisorption, sometimes to the point where it becomes exothermic. The

Table 1
The results of various kinds of interactions on Model I

No.	Initial close contact	Bond formed (distance in nm)	ΔE (kcal/mol)
1	C–Al_s interaction		
	C1–Al_s (Al_s^A or Al_s^B)	No reaction	
	C2–Al_s (Al_s^A or Al_s^B)	No reaction	
	C1–Al_s^A, C2–Al_s^A	No reaction	
	C1–Al_s^A, C2–Al_s^B	No reaction	
2	C–H_s interaction		
	C1–H_s (C = C1 or C2)	No reaction	
	C1–H_s, C2–H_s	No reaction	
3	C–O_s interaction		
	C1–O_s (O_s^A or O_s^B)	No reaction	
	C2–O_s (O_s^A or O_s^B)	No reaction	
	C1–O_s^C	C1–O_s^C (0.142)	84
	C2–O_s^C	C2–O_s^C (0.153)	105
4	H–O_s interaction		
	H–O_s (H = H1, H2, H3, or H6; $O_s = O_s^A$, O_s^B, or O_s^C)	No reaction	
5	C–O_s and H–O_s interaction		
	C1–O_s^A, H1–O_s^B	No reaction	
	C1–O_s^B, H1–O_s^A	No reaction	
	C1–O_s^C, H1–O_s^C	C1–O_s^C (0.139)	74
	C1–O_s^A, H2–O_s^B	C1–O_s^A (0.141), H2–O_s^B (0.096), H_s transfer	38
	C1–O_s^B, H2–O_s^A	C1–O_s^B (0.139), H2–O_s^A (0.104)	90
	C1–O_s^A, H2–O_s^C	No reaction	
	C1–O_s^C, H2–O_s^A	No reaction	
	C1–O_s^B, H2–O_s^C	C1–O_s^B (0.142), H2–O_s^C (0.098)	68
	C1–O_s^C, H2–O_s^B	C1–O_s^C (0.134), H2–O_s^B (0.097)	76
	C1–O_s^C, H2–O_s^C	C1–O_s^C (0.139), H2–O_s^C (0.103)	93
	C1–O_s^A, H3–O_s^B	C1–O_s^A (0.141), H3–O_s^B (0.096), H_s transfer	−12
	C1–O_s^A, H3–O_s^B	C1–O_s^A (0.144), H3–O_s^B (0.096)	38
	C1–O_s^B, H3–O_s^A	C1–O_s^B (0.142), H3–O_s^A (0.096), H_s transfer	−12
	C1–O_s^A, H3–O_s^C	C1–O_s^A (0.142), H3–O_s^C (0.097), H_s transfer	−4
	C1–O_s^A, H3–O_s^C	C1–O_s^A (0.148), H3–O_s^C (0.097)	29
	C1–O_s^C, H3–O_s^A	C1–O_s^C (0.146), H3–O_s^A (0.098)	47
	C1–O_s^B, H3–O_s^C	C1–O_s^B (0.142), H3–O_s^C (0.097)	4
	C1–O_s^C, H3–O_s^B	C1–O_s^C (0.146), H3–O_s^B (0.095)	19
	C1–O_s^C, H3–O_s^C	C1–O_s^C (0.140), H3–O_s^C (0.097)	38
	C2–O_s^A, H2–O_s^B	No reaction	
	C2–O_s^B, H2–O_s^A	C2–O_s^B (0.140), H2–O_s^A (0.095), H_s transfer	−1
	C2–O_s^C, H2–O_s^C	C2–O_s^C (0.140), H2–O_s^C (0.097)	66
	C2–O_s^C, H3–O_s^A	C1–O_s^C (0.141), H3–O_s^A (0.098)	40
	C2–O_s^C, H3–O_s^B	C1–O_s^C (0.145), H3–O_s^B (0.095)	15
	C2–O_s^C, H3–O_s^C	C1–O_s^C (0.140), H3–O_s^C (0.098)	37
6	C–Al_s and H–O_s interaction		
	C1–Al_s^B, H3–O_s^A	No reaction	
	C1–Al_s^B, H3–O_s^C	No reaction	
	C1–Al_s^A, H3–O_s^C	No reaction	
	C1–Al_s^A, H3–O_s^B	H3–O_s^B (0.096)	−63
7	C–O_s and C–O_s interaction		
	C1–O_s^A, C2–O_s^B	C1–O_s^A (0.140), C2–O_s^B (0.142), H_s transfer	11
	C1–O_s^B, C2–O_s^A	C1–O_s^B (0.140), C2–O_s^A (0.145), H_s transfer	11
	C1–O_s^C, C2–O_s^C	C1–O_s^C (0.144), C2–O_s^C (0.150)	58

ΔE, $E(\text{hexene}/H_8Al_{40}O_{64}) - E(\text{hexene}) - E(H_8Al_{40}O_{64})$.

optimized C–O_s bond lengths are all about 0.134–0.148 nm and H–O_s bond lengths about 0.095–0.104 nm. From the optimized C1–C2 (0.150–0.151 nm) and C2–C3 (0.134 nm) bond lengths, we can see that the double bond mainly locates at C2–C3 after chemisorption. All of the reactions are endothermic except for some cases in which H_s transfer occurs. The most energetically favorable reaction is H3 abstraction accompanied by the formation of a C1–O_s bond. This agrees with the suggestion of Trombetta et al. [5] that a hydrogen abstraction from the allylic position occurs, and gives rise to σ-bonded species. Our calculations find the species to be σ-bonded to an O center, however, not Al as suggested by Trombetta et al. [5] (Scheme 3). The

Table 2
Comparison of C–O and C=C stretching vibrational frequencies (in cm^{-1})

	1-Hexene		1-Butene	
	C1–O_s	C=C	C1–O_s	C=C
Frozen slab	928 (0.10), 939 (0.45)	1817 (0.00004)	940 (0.43)	1818 (0.0003)
Relaxed O_s	1146 (0.02)	1838 (0.00002)	1148 (0.0005)	1838 (0.0002)
Relaxed OAl_2	1147 (0.002), 1188 (0.17)	1839 (0.00004)	1156 (0.07)	1839 (0.0001)
Experimental [5]				1586, 1616

Data in parentheses are their intensities relative to the strongest peak in respective spectrum.

formation of a C–Al bond was proposed based on the fact that no IR absorption band around 1750–1650 or 1200–1000 cm^{-1} was found as would be expected in the presence of C=O or C–O bonds [5]. To compare with these IR observations, we calculated IR frequencies for the product of the C1–O_s^A and H3–O_s^B interaction (with H_s transfer). The calculated vibrational frequencies are 928 and 939 cm^{-1} for C1–O_s stretching and 1817 cm^{-1} for C2=C3 stretching. (see Table 2.) For these calculations the substrate was frozen, which has the effect of increasing the effective reduced mass associated with the vibrations, which in turn decreases the vibrational frequency. To refine this approximation, we repeated the structural optimization and frequency calculation of the product, allowing the O_s atom bound to C1 to move as well as the chemisorbed molecule. The predicted vibrational frequencies then become 1146 cm^{-1} for C1–O_s and 1838 cm^{-1} for C2=C3. It can be seen that additional freedom almost has no obvious effect on the C=C vibrational mode, but increases the C1–O_s frequency slightly while decreasing its intensity greatly. Taking the next logical step, we allowed the two Al atoms bound to O_s(−C1) to move as well. This yielded essentially no further change in the frequencies. Calculations of the corresponding vibrational frequencies for the chemisorbed state with C1–O_s^A and H3–O_s^B interactions between 1-butene and Model I gave almost the same results. For comparison, we also calculated the frequency of the C–O stretching mode in diethyl ether ($C_2H_5OC_2H_5$). The frequency is 1119 cm^{-1} with relative intensity 0.38, much higher than the computed intensities for the chemisorbed states. The low IR intensity for C1–O_s stretching may be the reason that C–O bands have not been observed experimentally [5]. Furthermore, compared to the experimental reports, our results overestimate the C=C stretching mode frequencies (1586 and 1616 cm^{-1}) by more than 200 cm^{-1}, which suggests that, in practice, the C–O frequency may be overestimated as well and therefore below the reported low-frequency edge of the observed IR spectrum (1100 cm^{-1}) [5]. Together with our study on C–Al interactions, these results suggest that the proposal that the new bond is a C–Al bond as opposed to a C–O bond merits further experimental scrutiny.

3.1.6. Simultaneous interactions of C with a surface Al and H with a surface O

For comparison, some configurations that bring C1 close to Al_s and H3 close to O_s were also tested. The results show that when C1 is placed close to Al_s^A and H3 close to O_s^B, H3 abstraction happens with the remnant radical leaving the surface. The energy difference of the final state from the free state ΔE is −63 kcal/mol, more exothermic than any reactions discussed above. This indicates that H3 abstraction is most favorable. As we have shown in Section 3.1.4, pure reactions between H and O_s cannot happen. Therefore, the interaction of C with Al_s promotes the H3 abstraction despite the observation that C–Al_s interaction is shown to be repulsive (Section 3.1.1). When we moved the fragment to the surface so that d(C1–Al_s^A) = 0.15 nm, the fragment leaves the surface again after full structural optimization.

3.1.7. Interactions of the C=C double bond with surface O atoms

Interactions between the C=C double bond and two surface O_s atoms were also investigated. The initial C1–O_s and C2–O_s distances are set to d(C–O_s) ≈ 0.16–0.17 nm. The results of full structural optimization are listed in Table 1. After optimization, the double bond is broken (d(C1–C2) = 0.160–0.161 nm) and both C1 and C2 bond to surface O atoms. The bond lengths of C1–O_s and C2–O_s are about 0.14–0.15 nm, with d(C1–O_s) slightly shorter than d(C2–O_s). The interaction with O_s^A causes the H_s to move to a nearby O_s. This kind of interaction is less favorable than the interaction of C1 and H3 with O_s.

3.2. Adsorption of hexene on Model II

From the results of our investigations of hexene adsorption on Model I, we can see that often H will be abstracted from the hexene molecule before anything else happens. Therefore, we studied only H–O_s interactions on Model II. Interactions of all six kinds of H atoms on hexene with a surface O_s atom were considered as indicated in Fig. 1(b). For all cases, the H atom was placed on top of the O_s and d(H–O_s) gradually decreased. It was found that all six kinds of H atoms can be dehydrogenated when d(H–O_s) is sufficiently short. The results are listed in Table 3, where the initial d(H–O_s) indicates the longest distance at which the reaction happens. In cases where two H atoms were dehydrogenated, they bonded to two different O_s atoms. The bond lengths of newly formed H–O_s bonds are all ≈0.095 nm. For the H1–O_s interaction, the H2 atom was also dehydrogenated, resulting in a triple bond. The results of H5–O_s and H6–O_s interactions are similar, where a new double bond was formed between C5 and C6. The energy difference of the final products may be due to the reaction of a second H on a different oxygen atom. For the H2–O_s and H3–O_s interactions, radicals were produced.

Table 3
The results of H–O_s interactions on Model II (distances in nm and energies in kcal/mol)

Interaction	Initial d(H–O_s)	Final abstracted H	Final d(C–C)	Product	ΔE	ΔE_{act}
H1–O_s	0.140	H1, H2	0.119 (C1–C2)	$CH{\equiv}CC_4H_9$	−152	13
H2–O_s	0.140	H2	0.129 (C1–C2), 0.143 (C2–C3)	$CH_2CC_4H_9$	−139	14
H3–O_s	0.155	H3	0.141 (C1–C2), 0.135 (C2–C3), 0.148 (C3–C4)	$CH_2CHCHC_3H_7$	−136	11
H4–O_s	0.145	H4	0.133 (C4–C5), 0.148 (C5–C6)	$CH_2{=}CHCH_2CH{=}CHCH_2$	−151	14
H5–O_s	0.150	H5, H6	0.149 (C4–C5), 0.133 (C5–C6)	$CH_2{=}CH(CH_2)_2CH{=}CH_2$	−105	12
H6–O_s	0.150	H5, H6	0.149 (C4–C5), 0.133 (C5–C6)	$CH_2{=}CH(CH_2)_2CH{=}CH_2$	−156	10

ΔE, E(hexene/$H_{10}Al_{50}O_{80}$)−E(hexene)−E($H_{10}Al_{50}O_{80}$); ΔE_{act}, activation energy of the reaction.

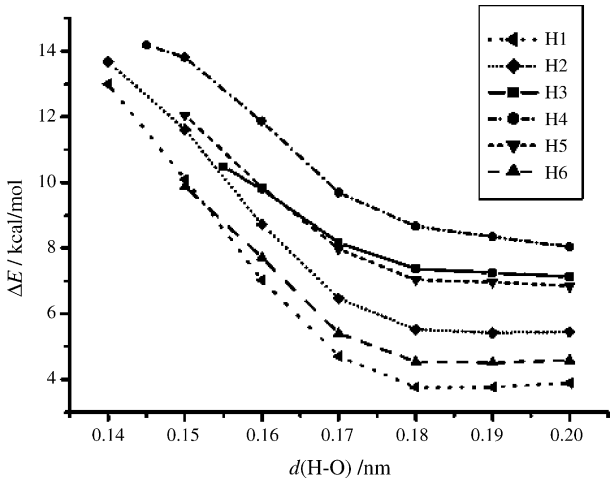

Fig. 4. Energy variations with H–O_s distance for hexene interactions with Model II. Note that these curves show the approach to the reaction barrier. The final chemisorbed states fall in the range $-156 \leq \Delta E \leq -105$ kcal/mol. Symbols indicate the computed points.

To see how much energy is required for these reactions to happen, we calculated the energy variation with the H–O_s distance by fixing the H atom at different positions from O_s and relaxing all other atoms in the molecule. (The H–O_s distance was varied from about 0.14 to 0.20 nm, in steps of 0.01 nm.) The results are shown in Fig. 4. It can be seen that the energy variation with H–O_s distance before reaction increases with the decrease of H–O_s distance. The energy barriers (ΔE_{act}) for the six reactions are around 10–15 kcal/mol (see Table 3), implying that there will be a plethora of products. We note that the design of a catalyst with high selectivity for a specific product reduces to modifying the catalyst to increase all but one of these barriers, potentially a significant challenge.

4. Conclusions

In conclusion, we have employed semi-empirical (PM3) cluster calculations to investigate the adsorption of 1-hexene on the γ-alumina (110C) surface. The results show that on the Al–O terminated surface, both C and H of hexene may form a bond to surface oxygen, but not to surface aluminum as has been proposed previously. The chemisorption is typically an endothermic process. The most preferable chemisorption involves the abstraction of H from the allylic position of hexene with or without the formation a C–O_s bond. On the oxygen-terminated surface, all kinds of H atoms on hexene can be abstracted by surface oxygen when they come sufficiently close to the surface. The energy barriers for these various H-abstraction steps are comparable, but are slightly lower for the dehydrogenation of a terminal H beyond the double bond or an allylic H than from other positions. These similar energy barriers suggest a possible reason for the experimentally observed plethora of products.

Acknowledgments

This work was supported in part by the USDOE under contract number DE-FC02-01CH11085, by an NSF GOALI Grant DMR-0111841 with Alcoa Inc., by DuPont and by NATO-PST-CLG-980354. The authors thank M. Caldararu and C. Horniou for valuable discussions of reaction mechanisms.

References

[1] H. Knozinger, P. Ratnasamy, Catal. Rev., Sci. Eng. 17 (1978) 31.
[2] C.N. Satterfield, Heterogeneous Catalysis in Practice, McGraw Hill, New York, 1980.
[3] S.E. Tung, E. Mcininch, J. Catal. 3 (1964) 229.
[4] S.E. Tung, E. McInninch, Proceedings of the 3rd International Congress on Catalysis, vol. 1, North Holland Publishing Company/New York Interscience Publishers, Amsterdam, 1965, pp. 687–710.
[5] M. Trombetta, G. Busca, S.A. Rossini, V. Piccoli, U. Cornaro, J. Catal. 168 (1997) 334.
[6] H. Tachikawa, T. Tsuchida, J. Mol. Catal. A, Chem. 96 (1995) 277.
[7] M.B. Fleisher, L.O. Golender, M.V. Shimanskaya, J. Chem. Soc., Faraday Trans. 87 (1991) 745.
[8] H. Kawakami, S. Yoshida, J. Chem. Soc., Faraday Trans. 81 (1985) 1117.
[9] O. Maresca, A. Allouche, J.P. Aycard, M. Rajzmann, S. Clemendot, F. Hutschka, J. Mol. Struct., Theochem. 505 (2000) 81.
[10] P. Hirva, T.A. Pakkanen, Surf. Sci. 277 (1992) 389.
[11] M. Lindblad, T.A. Pakkanen, Surf. Sci. 286 (1993) 333.
[12] D.A. De Vito, F. Gilardoni, L. Kiwi-Minsker, P.Y. Morgantini, S. Porchet, A. Renken, J. Weber, J. Mol. Struct., Theochem. 469 (1999) 7.
[13] S.H. Cai, K. Sohlberg, J. Mol. Catal. A, Chem. 193 (2003) 157.
[14] J.J.P. Stewart, J. Comput. Chem. 10 (1989) 209.
[15] J.J.P. Stewart, J. Comput. Chem. 10 (1989) 221.
[16] E.P. Smirnov, A.A. Tsyganenko, React. Kinet. Catal. Lett. 7 (1977) 425.
[17] E.P. Smirnov, A.A. Tsyganenko, React. Kinet. Catal. Lett. 26 (1984) 405.
[18] A.B.J. Parusel, W. Rettig, W. Sudholt, J. Phys. Chem. A 106 (2002) 804.
[19] E.D. Raczynska, M. Darowska, T. Rudka, M. Makowski, J. Phys. Org. Chem. 14 (2001) 770.
[20] P.U. Civcir, J. Mol. Struct., Theochem. 572 (2001) 5.

[21] A. Bere, J. Chen, A. Hairie, G. Nouet, E. Paumier, Comput. Mater. Sci. 17 (2000) 249.
[22] R.S. Zhou, R.L. Snyder, Acta Crystallogr. Sect. B, Struct. Sci. 47 (1991) 617.
[23] K. Sohlberg, S.J. Pennycook, S.T. Pantelides, J. Am. Chem. Soc. 121 (1999) 7493.
[24] Y. Chen, L.F. Zhang, Catal. Lett. 12 (1992) 51.
[25] P.D. Nellist, S.J. Pennycook, Science 274 (1996) 413.
[26] K. Sohlberg, S.J. Pennycook, S.T. Pantelides, J. Am. Chem. Soc. 121 (1999) 10999.
[27] L.J. Alvarez, J.F. Sanz, M.J. Capitan, M.A. Centeno, J.A. Odriozola, J. Chem. Soc., Faraday Trans. 89 (1993) 3623.
[28] D. Coster, A.L. Blumenfeld, J.J. Fripiat, J. Phys. Chem. 98 (1994) 6201.
[29] K. Sohlberg, S.T. Pantelides, S.J. Pennycook, J. Am. Chem. Soc. 123 (2001) 26.
[30] K. Sohlberg, S. Rashkeev, A.Y. Borisevich, S.J. Pennycook, S.T. Pantelides, ChemPhysChem 5 (2004) 1893.
[31] A.P. Scott, L. Radom, J. Phys. Chem. 100 (1996) 16502.
[32] R.H. Petrucci, General Chemistry: Principles and Modern Applications, Macmillan, New York, 1989.